

# ABA triblock copolymers containing polyhedral oligomeric silsesquioxane pendant groups: synthesis and unique properties

Jeffrey Pyun<sup>a,1</sup>, Krzysztof Matyjaszewski<sup>a,\*</sup>, Jian Wu<sup>b</sup>, Gyeong-Man Kim<sup>b</sup>,  
Seung B. Chun<sup>b,2</sup>, Patrick T. Mather<sup>b,\*</sup>

<sup>a</sup>Department of Chemistry, Center for Macromolecular Engineering, Carnegie Mellon University, 4400 Fifth Avenue, Pittsburgh, PA 15213, USA

<sup>b</sup>Polymer Program, Institute of Materials Science, University of Connecticut, Storrs, CT 06269-3136, USA

Received 4 November 2002; received in revised form 26 December 2002; accepted 9 January 2003

## Abstract

The synthesis and characterization of POSS containing ABA triblock copolymers is reported. The use of atom transfer radical polymerization (ATRP) enabled the preparation of well-defined model copolymers possessing a rubbery poly(*n*-butyl acrylate)(pBA) middle segment and glassy poly(3-(3,5,7,9,11,13,15-heptaisobutyl-pentacyclo[9.5.1.1<sup>3,9</sup>.1<sup>5,15</sup>.1<sup>7,13</sup>]-octasiloxane-1-yl)propyl methacrylate(p(MA-POSS)) outer segments. By tuning the relative composition and degree of polymerization (DP) of the two segments, phase separated microstructures were formed in thin films of the copolymer. Specifically, dynamic mechanical analysis and transmission electron microscopy (TEM) observations reveal that for a small molar ratio of p(MA-POSS)/pBA (DP = 6/481/6) no evidence of microphase separation is evident while a large ratio (10/201/10) reveals strong microphase separation. Surprisingly, the microphase-separated material exhibits a tensile modulus larger than expected (ca.  $2 \times 10^8$  Pa) for a continuous rubber phase for temperatures between a pBA-related  $T_g$  and a softening point for the p(MA-POSS)-rich phase. Transmission electron microscopy (TEM) images with selective staining for POSS revealed the formation of a morphology consisting of pBA cylinders in a continuous p(MA-POSS) phase. Thermal studies have revealed the existence of two clear glass transitions in the microphase-separated system with strong physical aging evident for annealing temperatures near the  $T_g$  of the higher  $T_g$  phase (p(MA-POSS)). The observed aging is reflected in wide-angle X-ray scattering as the strengthening of a low-angle POSS-dominated scattering peak, suggesting some level of ordering during physical aging. The  $T_g$  of the POSS-rich phase observed in the microphase separated triblock copolymer was nearly 25 °C higher than that of a POSS-homopolymer of the same molecular weight, suggesting a strong confinement-based enhancement of  $T_g$  in this system.

© 2003 Elsevier Science Ltd. All rights reserved.

**Keywords:** polyhedral oligomeric silsesquioxane; POSS; block copolymers

## 1. Introduction

The synthesis of linear organic/inorganic hybrid polymers containing polyhedral oligomeric silsesquioxane (POSS) groups has recently gained attention as a route to prepare novel nanocomposite materials [1]. In the pursuit to understand the effect of POSS inclusions in polymeric hybrids, the synthesis of well-defined model copolymers of precise molar mass, composition and architecture is required [2]. Numerous approaches have been reported in

the preparation of POSS containing copolymers, namely, condensation polymerization [3–5], ring-opening metathesis polymerization (ROMP) [6–8], metallocene-mediated processes [9] and free radical polymerization [10,11] techniques. Additionally, recent advances in controlled/living radical polymerization [12,13] have offered a versatile tool to prepare model copolymers from a wide range of monomers (e.g. styrenes, (meth)acrylates), enabling investigation of structure-property relationships [14]. Our group demonstrated the ability to introduce methacrylate functional POSS monomers into polyacrylate materials for the synthesis of well-defined star diblock and ABA triblock copolymers using atom transfer radical polymerization (ATRP) [15–18]. In these block copolymers, POSS moieties are attached to the copolymer backbone as pendant side chain groups.

\* Corresponding authors.

E-mail addresses: km3b@andrew.cmu.edu (K. Matyjaszewski), patrick.mather@uconn.edu (P. T. Mather).

<sup>1</sup> Present address: IBM, Almaden, CA, USA.

<sup>2</sup> Present address: Rogers Corporation, Rogers, CT, USA.

Several studies reported the presence of POSS groups to effect both thermal and rheological properties of polystyrene [19], polyurethane [4,20], polynorbornene [6, 7] and polypropylene-based blends and copolymers [9,21]. Limited findings on POSS-methacrylate copolymers have shown that high molecular weight POSS-containing homopolymers ( $M_w \sim 200$  kDa, DP  $\sim 100$ ) do not reveal a glass transition below thermal decomposition around  $T = 400$  °C [11]. However, systematic investigation of POSS-containing block copolymers based on poly(meth)acrylates has not been conducted. In particular, an ABA triblock copolymer composed of a soft polyacrylate middle segment and hard POSS based outer segments was of interest, as phase separation would yield sequestered domains of POSS groups on nanometer length scales. Such a system would allow examination of bulk morphology and properties due to POSS segments, but also may provide insight into the ordering of POSS groups within phase separated domains.

The effect of nano-confinement on organization within microphase separated domains of POSS-based copolymers is a phenomenon gaining increasing attention. While substantial work has been conducted on copolymers containing crystalline polymers with POSS segments, very limited attention has been given to the structure and morphology in block copolymers composed of amorphous segments with POSS groups [22]. Of particular interest is whether phase separated domains of POSS are crystalline, or glassy in nature. The POSS-rich phase may serve as physical crosslinks due to phase separation of glassy, or crystalline domains. There have been rare investigations on the physical aging behavior in 'pseudo' network systems [23]. We were prompted to question whether the glassy phase in our ABA block copolymer would exhibit the same behavior and properties relative to the analogous POSS containing homopolymers.

Herein, we report the synthesis and characterization of ABA triblock copolymers possessing a soft middle polyacrylate segment and POSS-containing outer blocks. By the use of ATRP we demonstrate the ability to prepare microphase separated structures by tuning composition and molar mass of each polymeric segment. Thermal analysis of the bulk copolymer using Differential Scanning Calorimetry (DSC), along with other complementary methods to also demonstrate how the presence of POSS domains affected morphology and properties of the hybrid material.

## 2. Experimental

### 2.1. Materials

*n*-Butyl acrylate (Acros) was stirred over calcium hydride overnight and distilled before use. Copper(I) bromide (Aldrich) and 4,4'-(di-5-nonyl)-2,2'-bipyridine (dNbpy) were purified and prepared according to previously reported

procedures [24]. Copper(II) bromide, *N,N,N',N'',N'''*-penta-methyldiethylenetriamine (PMDETA), dimethyl-2,7-dibromoheptanedioate were purchased from Aldrich and used as received. 3-(3,5,7,9,11,13,15-heptacyclopentyl-pentacyclo[9.5.1.1<sup>3,9</sup>.1<sup>5,15</sup>.1<sup>7,13</sup>]octasiloxane-1-yl)propyl methacrylate (cyclopentyl MA-POSS) and 3-(3,5,7,9,11,13,15-heptaisobutyl-pentacyclo[9.5.1.1<sup>3,9</sup>.1<sup>5,15</sup>.1<sup>7,13</sup>]octasiloxane-1-yl)propyl methacrylate (isobutyl MA-POSS) were purchased from Hybrid Plastics and used as received.

### 2.2. Characterization

- (i) *Size exclusion chromatography (SEC)*. Was performed in tetrahydrofuran using a Waters 510 pump, 3 Styragel columns (Polymer Standards Service, pore sizes  $10^5$  Å,  $10^3$  Å,  $10^2$  Å) and a Waters 2410 refractive index detector. Calculations of apparent molar mass were determined using the PSS software from a calibration based on linear polystyrene standards (from PSS).  $^1\text{H}$  NMR analysis was done on a 300 MHz Bruker spectrometer using the Tecmag software.
- (ii) *Dynamic Mechanical Analysis*. A TA Instruments 2980 DMA was run in tensile mode at an oscillation frequency of 1 Hz with a static force of 0.010 N, an oscillation amplitude of 5.0  $\mu\text{m}$  and an automatic tension of 125%. Samples were heated from  $T = -100$  °C (below  $T_g$  for pBA) to  $T = 100$  °C (above p(MA-POSS) softening) with a heating rate of 4 °C/min. The sample geometry was a thin film in tension.
- (iii) *Thermal Analysis*. The thermal properties of both POSS homopolymer and triblock copolymers were investigated using DSC with variation in thermal history so as to age the samples to varying degrees. For this purpose, a TA Instruments DSC 2920 was employed with samples (5–15 mg) prepared from powders and sealed in aluminum pans. Heating experiments were conducted with a nitrogen atmosphere and using a heating rate of 20 °C/min. For isolated cases a slower heating rate of 10 °C/min was employed with negligible differences observed. As our annealing periods extended to several days, annealing was performed on a custom-built hot-stage with temperature control to  $\pm 0.2$  °C.
- (iv) *Wide-Angle X-ray Scattering*. In order to assess microstructure and aging-induced microstructural changes in the POSS-triblock polymer, we have used wide-angle X-ray scattering (WAXS). For this purpose, we have employed a Bruker D5005 X-ray diffractometer with angular range  $5 < 2\theta < 40^\circ$  and using Cu  $K\alpha$  radiation with wavelength,  $\lambda = 1.5418$  Å. Samples were prepared as fine powders (after aging treatment) prior to WAXS data collection.
- (v) *Microscopy*. Investigations of morphology were performed using a Philips EM300 transmission electron microscope operated at 80 kV. Samples were cast from chloroform and the ultrathin sections for TEM with a thickness of about 50 nm were cryo-microtomed at

$T = -80\text{ }^{\circ}\text{C}$ . In order to increase the phase contrast the ultrathin sections were chemically selective vapor stained with  $\text{RuO}_4$ . Specifically, the ultra-thin sections of our triblock copolymer samples were transferred to 200 mesh copper grids and the sections placed in a glass jar containing 0.5%  $\text{RuO}_4$  aqueous solution. The sections were exposed to  $\text{RuO}_4$  vapor for 1–5 min, selectively staining the p(POSS-MA) block, believed to be easily stained owing to the high concentration of cyclopentyl groups. Selective staining of the POSS phase was determined by applying the same process to an immiscible blend of MA-POSS homopolymer and pMMA, with minor p(MA-POSS) content, and observing staining of the minor component with TEM. We assume that selectivity observed in this blend is the same for p(MA-POSS) and pBA, given compositional similarity.

- (vi) *Melt Rheology*. Investigations of linear viscoelastic behavior for a triblock copolymer showing microphase-separation were conducted using rotational rheometry (Rheometric Scientific ARES) for temperatures above the second softening (observed using DMA) to better understand the nature of this transition and the fluid properties. Samples were prepared by compression molding at  $T = 100\text{ }^{\circ}\text{C}$  with care taken to remove voids. The parallel plate geometry was adopted and frequency sweeps from  $\omega = 0.1\text{ rad/s}$  to  $\omega = 100\text{ rad/s}$  were conducted for temperatures spanning  $80\text{ }^{\circ}\text{C} < T < 170\text{ }^{\circ}\text{C}$ . Time-temperature superposition (TTS) was found to work moderately well over this temperature range without the use of vertical data shifting.

### 2.3. Synthesis of difunctional poly(*n*-butyl acrylate) macroinitiator ( $M_n = 61,700\text{ g/mol}$ )

To a 25 ml round bottom flask with magnetic stir bar was added  $\text{Cu(I)Br}$  (25 mg, 0.178 mmol),  $\text{Cu(II)Br}_2$  (2.0 mg, 0.009 mmol) and then the flask was fitted with a rubber septum. The reaction flask was then evacuated (1–5 mm Hg) and backfilled with nitrogen for three cycles. *n*-Butyl acrylate (20 ml, 139 mmol) was bubbled with nitrogen for 1 h before use and then added via syringe to the reaction vessel, followed by PMDETA (39  $\mu\text{l}$ , 0.187 mmol). To a separate 4 ml vial with magnetic stir bar was added dimethyl-2,6-dibromoheptanedioate (60 mg, 0.173 mmol). The vial was then fitted with a rubber septum and evacuated/backfilled with nitrogen (3 cycles). Nitrogen purged *n*-butyl acrylate (1 ml, 8.7 mmol) was then added via syringe to the vial to dissolve the initiator. The initiator solution was then transferred to the 25 ml round bottom flask containing the catalyst solution and the reaction vessel was placed in a  $70\text{ }^{\circ}\text{C}$  oil bath. The reaction was allowed to proceed for 16 hrs and 16 min.  $^1\text{H}$  NMR analysis of the polymerization mixture revealed that a monomer conversion of 57% was obtained. The polymer solution was diluted

in THF and filtered through neutral alumina to remove the catalyst. The polymer solution was then concentrated via distillation of THF in vacuo and precipitated into a ten-fold excess of methanol/water (4:1 by volume). SEC against linear pS standards indicated a molar mass of  $M_n = 61,700$ ;  $M_w/M_n = 1.31$ .

### 2.4. Synthesis of p(MA-POSS)-*b*-pBA-*b*-p(MA-POSS) from cyclopentyl functional POSS methacrylate monomer

To a 4 ml vial with magnetic stir bar was added 1 g of difunctional pBA macroinitiator ( $M_n = 61,700$ ), cyclopentyl MA-POSS (0.32 g, 0.3 mmol) and  $\text{Cu(I)Cl}$  (2.96 mg, 0.03 mmol). The vial was fitted with a rubber septum and deoxygenated by evacuation (1–5 mm Hg) and backfilling with nitrogen (3 cycles). PMDETA (6.26  $\mu\text{l}$ , 0.03 mmol) was then added via syringe and the reaction vessel was placed in an oil bath set at  $60\text{ }^{\circ}\text{C}$ . Polymerization allowed to proceed for 14 h and 32 min and  $^1\text{H}$  NMR analysis of the reaction mixture indicated that a monomer conversion of 90% was achieved. The polymer was then diluted in THF and passed through neutral alumina to remove catalyst. Following concentration of the polymer solution by in vacuo removal of THF, precipitation into a 10-fold excess of methanol/water (4:1 by volume) was conducted. Using this procedure, residual cyclopentyl MA-POSS could not be separated from the p(MA-POSS)-*b*-pBA-*b*-p(MA-POSS) triblock copolymer. Trituration of the crude product in 20 ml of nonane overnight at room temperature quantitatively removed MA-POSS monomer as confirmed by SEC.

### 2.5. Synthesis of poly(3-(3,5,7,9,11,13,15-heptaisobutyl-pentacyclo[9.5.1.1<sup>3,9</sup>.1<sup>5,15</sup>.1<sup>7,13</sup>]-octasiloxane-1-yl)propyl methacrylate (isobutyl MA-POSS) homopolymer

Isobutyl MA-POSS (1 g, 1.06 mmol) and AIBN (1.74 mg, 0.0106 mmol) were weighed into a 5 ml round bottom flask with magnetic stir bar. The flask was then fitted with a septum and was evacuated (1–5 mm Hg) and backfilled with nitrogen (3-cycles). Nitrogen purged (30 min) toluene (2 ml) was then added to the flask via syringe, and the flask was put into a  $60\text{ }^{\circ}\text{C}$  oil bath. Polymer was recovered by precipitation into methanol. The presence of residual monomer required fractionation of the higher molar mass homopolymer. Fractionation was conducted by dissolving 1 g of the p(MA-POSS)/MA-POSS crude mixture in 20 ml of THF, followed by the gradual addition of methanol. The first fraction was collected after the addition of 5 g of methanol. SEC analysis of the fractionated polymer revealed a molecular weight of  $M_n = 12,000\text{ g/mol}$  and a polydispersity of  $M_w/M_n = 1.8$ .

### 2.6. Synthesis of difunctional poly(*n*-butyl acrylate) macroinitiator ( $M_n = 25,800\text{ g/mol}$ )

To a 100 ml round bottom flask with magnetic stir bar

was added Cu(I)Br (50 mg, 0.35 mmol) and 1,4-dimethoxybenzene (1 g) and then the flask was fitted with a rubber septum. The reaction flask was then evacuated (1–5 mm Hg) and backfilled with nitrogen for three cycles. *n*-Butyl acrylate (50 ml, 349 mmol) was bubbled with nitrogen for 1 h before use and then added via syringe to the reaction vessel, followed by PMDETA (60 mg, 0.35 mmol) and dimethyl-2,6-dibromoheptanedioate (603 mg, 1.745 mmol). The reaction vessel was placed in an 80 °C oil bath. The reaction was allowed to proceed for 3 hrs and 39 min. <sup>1</sup>H NMR analysis of the polymerization mixture revealed that a monomer conversion of 91% was obtained. The polymer solution was diluted in THF and filtered through neutral alumina to remove the catalyst. The polymer solution was then concentrated via distillation of THF under vacuum and precipitated into a ten-fold excess of methanol/water (4:1 by volume). SEC against linear polystyrene standards indicated a molar mass of  $M_n = 25,800$ ;  $M_w/M_n = 1.20$ .

### 2.7. Synthesis of *p*(MA-POSS)-*b*-*p*BA-*b*-*p*(MA-POSS) from isobutyl functional POSS methacrylate monomer

To a 10 ml Schlenk flask with magnetic stir bar was added isobutyl MA-POSS (1.27 g, 1.34 mmol) and Cu(I)Cl (1.4 mg, 0.014 mmol). The flask was then fitted with a rubber septum and deoxygenated by evacuation (1–5 mm Hg) and backfilling with nitrogen (3 cycles). To a separate vial was added difunctional *p*BA macroinitiator ( $M_n = 25,800$  g/mol) (1 g, 0.03 mmol Br) and then a rubber septum was fitted over the vial. Deoxygenation of the vial was performed by evacuation (1–5 mm Hg) and backfilling with nitrogen (3 cycles). *o*-Xylene (2.5 ml) was bubbled with nitrogen for 1 hr before use and then added to the vial via syringe. The *p*BA macroinitiator solution was then transferred to the 10 ml Schlenk flask via syringe. PMDETA (3.6  $\mu$ l, 0.014 mmol) was added to reaction vessel via microliter syringe and the flask was placed in an oil bath set to 60 °C for 22 h and 54 min. Monomer conversion was determined via <sup>1</sup>H NMR and proceeded to 90%. The product was then diluted in 5 ml of THF and precipitated into 100 ml of methanol. To remove residual isobutyl MA-POSS monomer, ultrafiltration was employed using the Millipore Solvent Resistant Stirred Cell (XFUF 07601). The crude triblock copolymer of *p*(MA-POSS)-*b*-*p*(BA)-*p*(MA-POSS) was dissolved in toluene (120 ml) and methanol (60 ml). Ultrafiltration at 15–20 psig of nitrogen using RC filters (MWCO 100,000, Millipore, PLGC07610) was done for 60 min until approximately 50 ml of the solution remained. The solution from the cell was decanted and allowed to dry first in air, then under vacuum. After drying, 750 mg of the triblock copolymer was recovered. SEC against linear *p*S standards was used to determine molar mass ( $M_n = 43,010$  g/mol;  $M_w/M_n = 1.20$ ) of the triblock copolymer and confirmed quantitative removal of the POSS monomer.

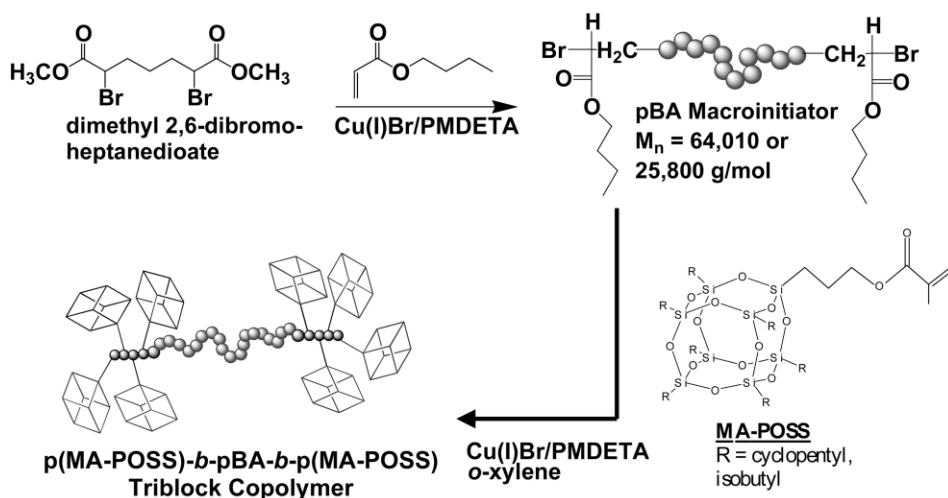
## 3. Results and discussion

### 3.1. Synthesis of ABA triblock copolymers using ATRP

The synthesis of ABA triblock copolymers possessing a central segment of poly(*n*-butyl acrylate)(*p*BA) and outer blocks of poly(methacryate-POSS)(*p*(MA-POSS)) was conducted using a two-step ATRP strategy [16]. Compositions of approximately 10–20 wt% of *p*(MA-POSS) were targeted for the design of a spherical morphology of phase separated *p*(MA-POSS) domains in a matrix of *p*BA. In the first stage of the synthesis, the ATRP of *n*-butyl acrylate (BA) was conducted using dimethyl-2,6-dibromoheptanedioate as the initiator for the preparation of a difunctional *p*BA macroinitiator (Scheme 1). To retain high chain end functionality, the polymerization was stopped at 57% monomer conversion (<sup>1</sup>H NMR) while targeting a high degree of polymerization ( $[M]_o/[I]_o = 800$ ). SEC of the macroinitiator relative to linear *p*S standards was used to calculate molar mass ( $M_n = 61,700$  g/mol;  $M_w/M_n = 1.31$ ). Comparison of theoretical molar mass values based on conversion and the ratio of monomer to initiator (i.e.  $M_n^{\text{theoretical}} = \text{conversion} \times ([M]_o/[I]_o) \times MW_{\text{BA}} = 58,400$  g/mol) versus those from SEC ( $M_n^{\text{SEC}} = 61,700$  g/mol) indicated that an initiation efficiency in the polymerization was 94%.

Chain extension of the *p*BA macroinitiator was then conducted by the ATRP of 3-(3,5,7,9,11,13,15-heptacyclopentyl-pentacyclo[9.5.1.1<sup>3,9</sup>.1<sup>5,15</sup>.1<sup>7,13</sup>]octasiloxane-1-yl)propyl methacrylate (cyclopentyl MA-POSS). In the ATRP reaction, a monomer conversion of 92% was achieved, as determined from <sup>1</sup>H NMR. SEC of the triblock copolymer against linear *p*S standards confirmed a small increase in molar mass ( $M_n = 64,010$ ;  $M_w/M_n = 1.39$ ) after the ATRP of cyclopentyl MA-POSS. Composition of the triblock copolymer and  $DP_n$  of each segment was determined via <sup>1</sup>H NMR in conjunction with corrected  $M_n^{\text{SEC}}$  values of the *p*BA macroinitiator (2.5 mol%; 16 wt% of *p*(MA-POSS)). The overall molar composition of the triblock copolymer was determined to be *p*(MA-POSS)<sub>6</sub>-*b*-*p*BA<sub>481</sub>-*b*-*p*(MA-POSS)<sub>6</sub>.

Initial morphological investigations of thin films prepared from the *p*(MA-POSS)<sub>6</sub>-*b*-*p*BA<sub>481</sub>-*b*-*p*(MA-POSS)<sub>6</sub> triblock copolymer was conducted using small angle X-ray scattering (SAXS) and (TEM). Both techniques confirmed that morphology of triblock copolymer thin films were featureless, indicating that phase separation was not induced at this composition and molar mass. Efforts to prepare phase-separated structures by increasing the  $DP_n$  of the *p*(MA-POSS) were not successful, as limiting degrees of polymerization were observed in the ATRP of MA-POSS monomers ( $DP_n < 15$ ) [16]. This observation is consistent with similar reports of limiting DP in the ROMP of dendritic macromonomers, presumably due to inaccessibility of the ruthenium complexed chain-ends shielded by bulky dendron side chain groups [25]. Thus, in the ATRP of



Scheme 1. Synthetic methodology for the preparation of ABA triblocks containing a poly(*n*-butyl acrylate) middle segments and outer segments of p(MA-POSS). In the first step, difunctional pBA macroinitiator is prepared by the ATRP of BA from a dimethyl 2,6-dibromoheptanedioate initiator. Subsequent chain extension of the pBA macroinitiator with MA-POSS yielded the ABA triblock copolymer.

MA-POSS monomers, bromine-end groups from growing p(MA-POSS) chains may also be inaccessible to copper(I) complexes after a certain DP is reached in the polymerization.

An alternative approach to preparing phase-separated microstructures was devised by preparing a difunctional pBA macroinitiator of lower molar mass. While the overall  $DP_n$  of the block copolymer was reduced, decreasing the relative composition (i.e. volume fraction,  $f_a$ ) of pBA to p(MA-POSS) segments was anticipated to yield phase-separated morphologies assuming large values for the interaction parameter ( $\chi$ ) [26]. Additionally, the isobutyl MA-POSS monomer was chosen in this case over the cyclopentyl MA-POSS due to observation of a clear glass transition in isobutyl p(MA-POSS) homopolymer, as will be discussed in later sections.

The synthetic route to prepare phase separated materials was similar to that used for the higher molar mass POSS triblock, except a lower monomer to initiator ratio ( $[M]_0/[I]$ ) was employed in the ATRP of BA for the synthesis of the difunctional macroinitiator. The polymerization of BA reached a conversion of 90% and SEC relative to pS standards confirmed the synthesis of lower molar mass pBA ( $M_n = 25,800$ ;  $M_w/M_n = 1.20$ ). A high initiation efficiency (>90%) was also observed in the polymerization as for the higher molar mass pBA macroinitiator. Chain extension of the macroinitiator with 3-(3,5,7,9,11,13,15-heptaisobutylpentacyclo-[9.5.1.1<sup>3,9</sup>.1<sup>5,15</sup>.1<sup>7,13</sup>]octasiloxane-1-yl)propyl methacrylate (isobutyl MA-POSS) was then conducted and proceeded to high conversion (92%) as measured using  $^1\text{H}$  NMR. Monomer conversion was determined by monitoring consumption of vinyl protons ( $\delta = 6.10, 5.50$  ppm) from isobutyl MA-POSS relative to resonances from pBA macroinitiator protons.

$^1\text{H}$  NMR of the p(MA-POSS)-b-pBA-b-p(MA-POSS) triblock copolymer purified by ultrafiltration indicated the

presence of protons from both *n*-butyl and POSS side chain groups. Resonances from the poly(meth)acrylate backbone ( $\delta = 0.7\text{--}2$  ppm) were poorly resolved due to the abundance of protons from side chain groups, with the exception of methine protons ( $\delta = 2.35$  ppm, 6, Fig. 1) from the pBA segment. Resonances observed at  $\delta = 0.60$  ppm (1 and 4, Fig. 1) were clearly assigned to methylene protons from p(MA-POSS) segments. Methyl protons ( $\delta = 1.0$  ppm, 2, Fig. 1) and methine protons ( $\delta = 1.95$  ppm, 2, Fig. 1) from isobutyl groups in p(MA-POSS) were distinguishable in addition to methyl protons ( $\delta = 1.0$  ppm, 10, Fig. 1) and methylene groups from *n*-butyl groups in the pBA macroinitiator ( $\delta = 1.5$  and 1.8 ppm, 9 and 10 Fig. 1). At higher chemical shift, methylene protons from both pBA ( $\delta = 4.0$  ppm, 7, Fig. 1) and p(MA-POSS) ( $\delta = 3.8$  ppm, 5, Fig. 1) were observed indicating successful chain extension had occurred. Calculations of molar composition of each component was conducted by comparison of integration from p(MA-POSS) methylene protons ( $\delta = 0.60$  ppm, 1 and 4, Fig. 1) and pBA methine protons ( $\delta = 2.35$  ppm, 6, Fig. 1). Overall, the composition of p(MA-POSS) from  $^1\text{H}$  NMR was determined to be 9.7 mol%, corresponding to 44 wt%. The  $DP_n$  was also calculated, beginning from  $M_n$  SEC values of the pBA macroinitiator ( $M_n = 25,800$  g/mol) yielding molar ratios, of p(MA-POSS)<sub>10</sub>-b-pBA<sub>201</sub>-b-p(MA-POSS)<sub>10</sub> for the final triblock copolymer. This corresponds to a SEC-determined composition of 9.1 mol% and 42.4 wt% of p(MA-POSS). Thus, both estimations of the triblock copolymer composition ( $^1\text{H}$  NMR and SEC) yield a substantial POSS weight fraction that we expected to strongly modify morphological and rheological properties relative to the lower POSS-content triblock with 16 wt% p(MA-POSS).

SEC of the triblock copolymer against linear pS standards confirmed the incorporation of p(MA-POSS) as a small but clear increase in molar mass ( $M_n = 43,010$ ;

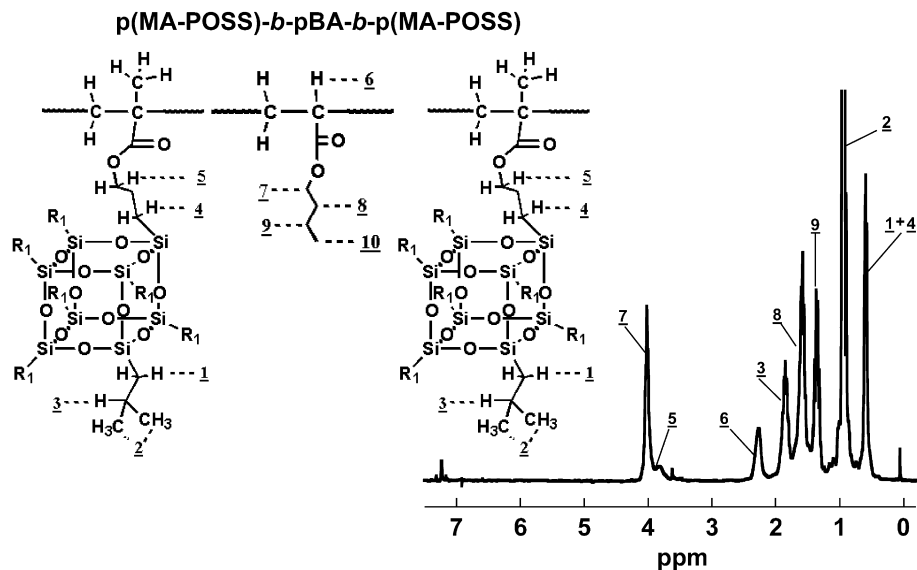


Fig. 1.  $^1\text{H}$  NMR spectrum of  $\text{p(MA-POSS)}_{10}\text{-}b\text{-pBA}_{201}\text{-}b\text{-p(POSS-MA)}_{10}$  with peak assignments as shown.

$M_w/M_n = 1.20$ ) relative to the macroinitiator was obtained (Fig. 2). Importantly, low polydispersity was observed for ATRP chain extension of the pBA macroinitiator with MA-POSS.

### 3.2. DMA observation of melt-pressed triblocks of varying PBA molecular weight

To begin our characterization comparison of the two triblocks, we conducted DMA temperature sweeps on tensile specimens, the results being shown in Fig. 3. Such measurements are sensitive to changes in thermal transitions, observed through loss tangent peaks, and are connected to morphology differences through storage modulus magnitude. Comparison of the DMA spectra

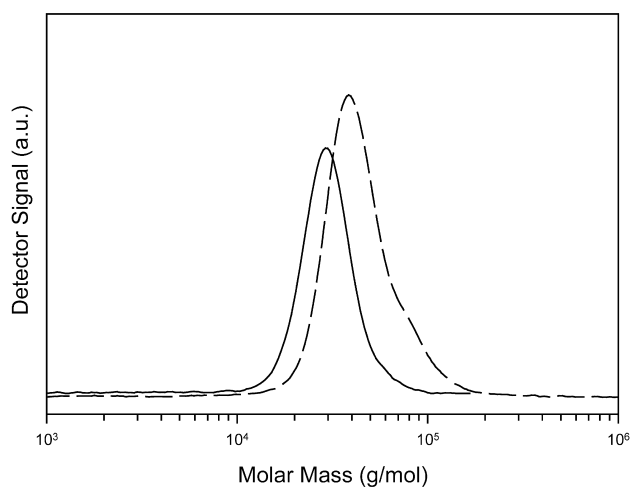


Fig. 2. Representative size exclusion chromatogram (SEC) of pBA macromonomer (solid line) and  $\text{p(MA-POSS)}_{10}\text{-}b\text{-pBA}_{201}\text{-}b\text{-p(POSS-MA)}_{10}$  (dashed line). Molar mass scale is computed from elution volume using polystyrene calibration standards and solution refractive index was used as the detection scheme.

between the higher molar mass  $\text{p(MA-POSS)}_6\text{-}b\text{-pBA}_{481}\text{-}b\text{-p(MA-POSS)}_6$  (trace (i)) and the  $\text{p(MA-POSS)}_{10}\text{-}b\text{-pBA}_{201}\text{-}b\text{-p(MA-POSS)}_{10}$  (trace (ii)) copolymers also provided greater insight into the organization of p(MA-POSS) segments in the microphase separated system. For the homogeneous  $\text{p(MA-POSS)}_6\text{-}b\text{-pBA}_{481}\text{-}b\text{-p(MA-POSS)}_6$  system, a plateau tensile modulus above the  $T_g$  of pBA of

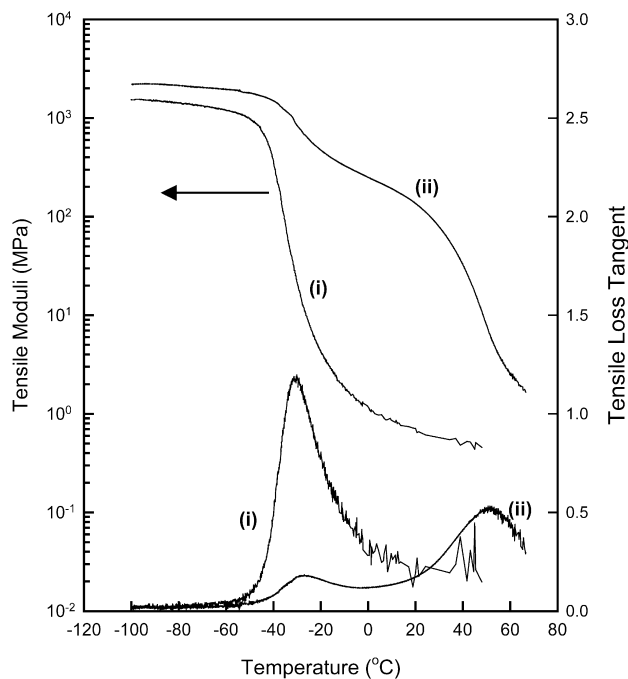


Fig. 3. Dynamic Mechanical Analysis (DMA) comparing POSS-triblocks of varying poly(butyl acrylate) central block molecular weight: (i)  $\text{p(MA-POSS)}_6\text{-}b\text{-pBA}_{481}\text{-}b\text{-p(MA-POSS)}_6$  and (ii)  $\text{p(MA-POSS)}_{10}\text{-}b\text{-pBA}_{201}\text{-}b\text{-p(POSS-MA)}_{10}$ . Tensile films were prepared by solvent casting and temperature sweeps conducted at a heating rate of  $4\text{ }^\circ\text{C}/\text{min}$  while applying oscillatory strain of approximate magnitude 0.1% and with a frequency of 1 Hz.

approximately 0.4 MPa was observed. Taking the glass transition temperature to be the onset of tensile modulus decrease (for comparison with DSC) we measure a value of  $T_g = -48\text{ }^\circ\text{C}$  for the high molecular weight sample (trace (i)) and  $T_g = -42\text{ }^\circ\text{C}$  for the lower molecular weight (trace (ii)). We note that the entanglement molecular weight for pure pBA has been reported [27] to be 28,000 g/mol (substantially larger than the 8,800 value for pMA [28,29]), from which we have estimated the plateau modulus in shear,  $G_N^0$ , to 0.1 MPa or 0.3 MPa in tension. By comparing our observed value with that estimated from  $M_e$  measurements of others [27], we reason that this material behaves as an ordinary entangled poly(*n*-butyl acrylate).

For the phase separated p(MA-POSS)<sub>10</sub>-*b*-pBA<sub>201</sub>-*b*-p(MA-POSS)<sub>10</sub> sample, however, a significantly higher plateau modulus was observed (200 MPa) in the same temperature range as for the homogeneous system. The large difference in the plateau moduli of the two copolymer systems cannot be solely attributed to an increase in the physical crosslink density due to microphase separation of p(MA-POSS) domains in a matrix of pBA. Instead, the enhanced value of the plateau modulus suggests the formation of a microphase separated structure (to be clarified by TEM) composed, surprisingly, of a continuous phase of solid p(MA-POSS) -glassy or semicrystalline - and dispersed domains of pBA. The inverse morphology would be expected to yield a much lower tensile modulus  $\sim 1$  MPa. This assessment is further supported by the larger magnitude of the loss tangent transition at 70 °C relative to the value at  $-30\text{ }^\circ\text{C}$ . Assignments of these transitions correspond to the  $T_g$  of the pBA phase at  $-30\text{ }^\circ\text{C}$  and softening of the p(MA-POSS) phase at 50 °C. Furthermore, the effect of a larger weight fraction of POSS in the p(MA-POSS)<sub>10</sub>-*b*-pBA<sub>201</sub>-*b*-p(MA-POSS)<sub>10</sub> copolymer was also seen in the DMA by doubling of the cryogenic modulus (below  $T_g$  of pBA) relative to the p(MA-POSS)<sub>6</sub>-*b*-pBA<sub>481</sub>-*b*-p(MA-POSS)<sub>6</sub> sample, which is consistent with previous reports for random copolymer systems containing POSS [6]. Finally, no significant difference in the pBA-rich  $T_g$  is observed for the two block copolymers, indicating a negligible influence of POSS on pBA softening in either the single or two phase systems.

As we will show below, these results are consistent with TEM analysis and limited SAXS observations (data not shown) for the two triblock copolymer systems. Collectively, these characterization data reveal that microphase separated structures can be formed by optimizing the length of central pBA block provided the DP of p(MA-POSS) block is constant.

### 3.3. Morphology of POSS triblock copolymer thin films

Morphological investigations of p(MA-POSS)<sub>6</sub>-*b*-pBA<sub>481</sub>-*b*-p(MA-POSS)<sub>6</sub> triblock copolymer thin films prepared with pBA macroinitiator of higher molar mass ( $M_{n, SEC} = 64,010$ ;  $M_w/M_n = 1.39$ ) by using SAXS and

TEM indicated that no microphase separation was induced during sample preparation; i.e. the resulting morphology and SAXS scattering patterns were completely featureless. However, the morphology of p(MA-POSS)<sub>10</sub>-*b*-pBA<sub>201</sub>-*b*-p(MA-POSS)<sub>10</sub> triblock copolymer thin films prepared with a difunctional pBA macroinitiator of lower molar mass ( $M_{n, SEC} = 25,800$  g/mol;  $M_w/M_n = 1.20$ ) show remarkably well-defined microphase separated structures. In Fig. 4, we show typical microphase separated block copolymer structures imaged by TEM by employing ultrathin sections of thickness  $\sim 50$  nm that were stained with RuO<sub>4</sub> vapor. In a relatively low magnification TEM image (Fig. 4a), well-defined white cylinders are clearly discerned to be oriented both in and out of the sample plane. In our previous TEM studies on POSS incorporated thermosets, we found that the POSS moiety can be selectively stained with RuO<sub>4</sub>, although the chemical details of this staining have not been revealed [30]. On this basis, we are confident that the continuous dark phase consists of the p(MA-POSS) block, whereas the bright cylinders consist of pBA. The micrographs of Fig. 4(b) and (c) show higher magnification imaging of local areas in Fig. 4(a). The bright domains originating from pBA are locally well ordered in dark continuous p(MA-POSS) matrix phase, but macroscopically disordered. The fast Fourier transform (FFT) power

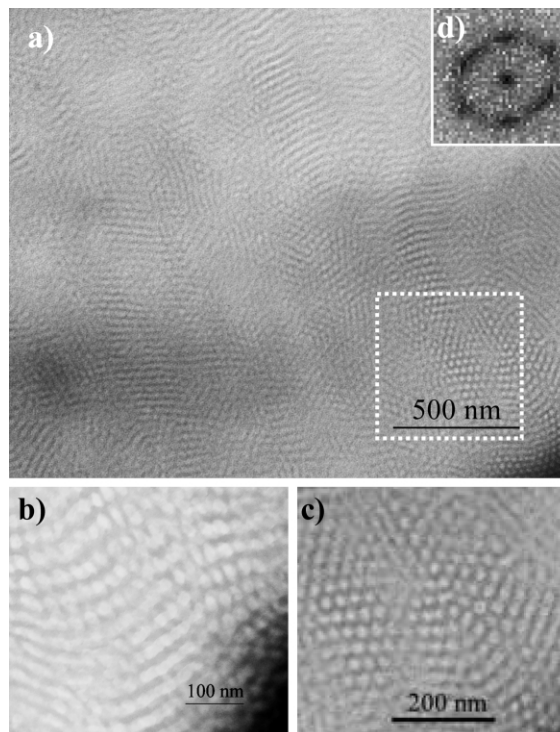


Fig. 4. Transmission electron microscopy (TEM) of thin sections of POSS-triblocks prepared with cryomicrotomy at  $T = -80\text{ }^\circ\text{C}$  to yield samples of thickness  $\sim 50$  nm. The microtomed sections were chemically treated with RuO<sub>4</sub>, an agent selective for POSS. (a) Low magnification micrograph showing overall morphology, (b)–(c) Higher magnification micrographs revealing cylindrical morphology, (d) Fourier transform of selected area from micrograph (a) revealing symmetry consistent with local hexagonal packing of the cylinders.

spectrum was computed (Fig. 4(d)) for a portion of Fig. 4(a) showing cylinders aligned normal to the sample plane, revealing six strong spots due to a three-fold symmetrical arrangement of pBA domains within the p(MA-POSS) matrix phase. Thus it appears that pBA cylinders are dispersed in a p(MA-POSS) matrix despite the latter being a slightly minor component on a weight fraction basis, thus favoring lamellae formation. In particular,  $^1\text{H}$  NMR characterization revealed that the overall fraction p(MA-POSS) within the triblock was 9.7 mol%, but 44 wt%. This surprising observation is perhaps attributed to unique excluded volume effects of p(MA-POSS) phase in this type of ABA block copolymer.

### 3.4. Thermal analysis of POSS homopolymers and triblock copolymers

Previous studies in the DSC of cyclopentyl- and cyclohexyl-substituted POSS homopolymers reported onset of decomposition occurring before observation of the glass transition ( $T_g$ ) [10,11]. This phenomenon was ascribed to retardation of segmental motion of polymer chains due to presence of bulky side chain groups at each repeat unit of the backbone [19]. In addition, a previous study [22] on diblock copolymers of polynorbornene and poly(norbornene-POSS) showed that increasing the length of the PN-POSS block had no effect on the polynorbornene-rich phase  $T_g$ , with  $T_g \sim 55^\circ\text{C}$ , while the morphologies traverse the usual sequence of spheres-cylinders-lamellae. However, a  $T_g$  was not detected for the POSS-PN phase for temperature below decomposition. In the present study, we have found that for the single-phase system, p(MA-POSS)<sub>6</sub>-b-pBA<sub>481</sub>-b-p(MA-POSS)<sub>6</sub>, a single  $T_g \sim -50^\circ\text{C}$  is observed (data not shown), essentially unmodified from pure pBA homopolymer. Above this temperature, the p(MA-POSS)<sub>6</sub>-b-pBA<sub>481</sub>-b-p(MA-POSS)<sub>6</sub> copolymer behaves as an entangled polyacrylate (Fig. 3). Thus, in the single phase case, we observe simple glass-rubber transition behavior. In contrast, for the p(MA-POSS)<sub>10</sub>-b-pBA<sub>201</sub>-b-p(MA-POSS)<sub>10</sub> triblock copolymer, we observed remarkably different phase behavior that is reflected in the DMA response (Fig. 3) and in DSC results we now present.

By comparison, the thermal transition behavior of p(MA-POSS)<sub>10</sub>-b-pBA<sub>201</sub>-p(MA-POSS)<sub>10</sub> is quite sensitive to thermal history, but generally shows two strong transitions. As shown in Fig. 5, trace (i), near  $T = -48^\circ\text{C}$  (onset), we observe a strong  $T_g$  signal indicated by a dramatic step in heat capacity at that temperature. This temperature is to be compared with the  $T_g$  for pure pBA of  $T = -54^\circ\text{C}$  [31]. Less obvious is a second transition with an onset of  $T = 65^\circ\text{C}$  ( $\Delta H = 0.71\text{ J/g}$ ) that appears to be first order melting during the first heating of the as-synthesized (and precipitated) powder. However, we were surprised to find a melting transition for a p(MA-POSS) rich phase at such a low temperature, or even at all, based on prior reports on POSS containing homopolymers showing the absence of

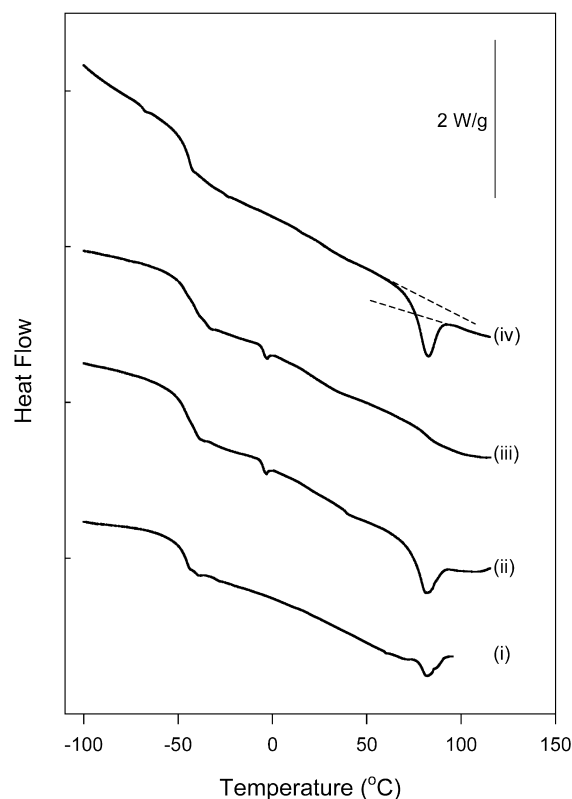


Fig. 5. Differential Scanning Calorimetry (DSC) characterization of triblock copolymer p(MA-POSS)<sub>10</sub>-b-pBA<sub>201</sub>-b-p(MA-POSS)<sub>10</sub> using a heating rate of  $20^\circ\text{C}/\text{min}$  for the following thermal history: (i) The first scan (after cooling to  $T = -100^\circ\text{C}$ ); (ii) Heating scan following (i) and direct cooling to  $T = 45^\circ\text{C}$  for 40 hours of annealing and subsequent cooling at  $20^\circ\text{C}/\text{min}$  to  $T = -100^\circ\text{C}$ ; (iii) heating scan after (ii); (iv) Heating scan following (iii) and direct cooling to  $T = 45^\circ\text{C}$  for 7 days of annealing and subsequent cooling at  $20^\circ\text{C}/\text{min}$  to  $T = -100^\circ\text{C}$  for reheating.

crystallization. Therefore, we sought to determine whether or not this observation was a true melting point, a first heating artifact, or the manifestation of significant physical aging present in the POSS phase. If the latent heat feature of Fig. 5(i) could be enhanced via thermal treatment at  $T < 65^\circ\text{C}$  or removed by quenching to leave a strictly second-order transition, then physical aging would be implicated. Thus, following the first heating scan, the triblock copolymer sample was cooled to  $T = 45^\circ\text{C}$  and annealed at that temperature for 40 hours under nitrogen and then re-scanned from  $T = -100^\circ\text{C}$  to  $100^\circ\text{C}$  as shown in Fig. 5(ii). We observed that this thermal history enhanced the latent heat endotherm while maintaining the transition temperature beginning near  $65^\circ\text{C}$ . However, the DSC trace of this annealed sample has further revealed a significant heat capacity offset above and below the thermal transition, an aspect discussed further below.<sup>3</sup> In light of this annealing-induced enhancement of the latent endotherm at  $T_g$ , we consider the endotherm itself as a reflection of

<sup>3</sup> We note that the slight fluctuation in the DSC thermogram at  $T = 0^\circ\text{C}$  was an artifact of our DSC for those runs.

enthalpy relaxation that occurred during significant physical aging at  $T = 45^\circ\text{C}$ .

Following this heating run, the sample was again cooled to  $T = -100^\circ\text{C}$ , this time without intermediate aging. In this case, trace (iii), two clear  $T_g$  transitions are observed with the following onset temperatures:  $T_g^{\text{pBA}} = -52^\circ\text{C}$  and  $T_g^{\text{pMA-POSS}} = 75^\circ\text{C}$ .  $T_g^{\text{pBA}}$ , associated with the softening of the pBA-rich phase is about 3–4  $^\circ\text{C}$  lower than the value measured in trace (i) (virgin sample) and features a larger step change in heat capacity, although we have not investigated this change quantitatively. More importantly, no latent heat endotherm is observed at  $T_g^{\text{pMA-POSS}}$  in this case, revealing the lack of enthalpy relaxation during prior cooling to  $T = -100^\circ\text{C}$ . Finally, the triblock copolymer was cooled to  $T = 45^\circ\text{C}$  for long duration annealing (7 days) to see if the physical aging associated with trace 5 (ii) could be reproduced. The resulting heating scan (trace iv) revealed pBA glass transition as before and a latent heat endotherm at the pMA-POSS  $T_g$  with an onset at  $T = 65^\circ\text{C}$  and a peak at  $T = 82.3^\circ\text{C}$  ( $\Delta H = 1.64\text{ J/g}$ ), but with an obvious step in heat capacity across the transition. We note that DMA experiments (Fig. 3) were performed on unaged specimens so that comparison between Fig. 3, trace (ii) should be made with Fig. 5, trace (i). We further note that the DMA data show a slightly lower temperature for the second transition.

To our knowledge, the phenomena observed in Fig. 5 are thus far unique for POSS-based systems in revealing a clearly detectable glass transition for a POSS homopolymer phase, albeit within a microphase morphology. Thus, we were prompted to examine the thermal response of a p(MA-POSS) homopolymer of similar molecular weight to that of the block contained in the p(MA-POSS)<sub>10</sub>-b-pBA<sub>201</sub>-b-p(MA-POSS)<sub>10</sub> triblock. Does such a polymer reveal an accessible glass transition in contrast to p(MA-POSS) homopolymers with cyclopentyl or cyclohexyl [11] corner groups? The DSC results for such a p(MA-POSS) homopolymer with  $M_n = 12,000\text{ g/mol}$  ( $M_w/M_n = 1.7$ ) are shown in Fig. 6, this time focusing on a single transition observed near  $T = 60^\circ\text{C}$ . Specifically, the first scan of the precipitated polymer sample, trace a (i), reveals a strong endotherm at  $T = 63.6^\circ\text{C}$  with  $\Delta H = 1.76\text{ J/g}$ . A second scan taken immediately after cooling to  $T = 0^\circ\text{C}$  (trace a (ii)) shows reduction of this complex transition to a simple glass transition with a low onset  $T_g = 40.5^\circ\text{C}$ . We immediately see that  $T_g$  of the POSS homopolymer is significantly lower ( $\Delta T_g \sim 25^\circ\text{C}$ ) than that of the POSS-rich phase in the p(MA-POSS)<sub>10</sub>-b-pBA<sub>201</sub>-b-p(MA-POSS)<sub>10</sub> triblock copolymer. Following this thermal history, enthalpy relaxation was attempted by annealing the sample at  $T = 45^\circ\text{C}$  (like for the triblocks in Fig. 5), for four days, the resulting heating scan being shown as trace b (i) in Fig. 6. Clearly, no latent heat endotherm is observed to indicate enthalpy relaxation, but instead a simple  $T_g$  is observed at  $47^\circ\text{C}$ . A second heat with no intervening heat treatment (trace b (ii)) shows no alteration of the thermal

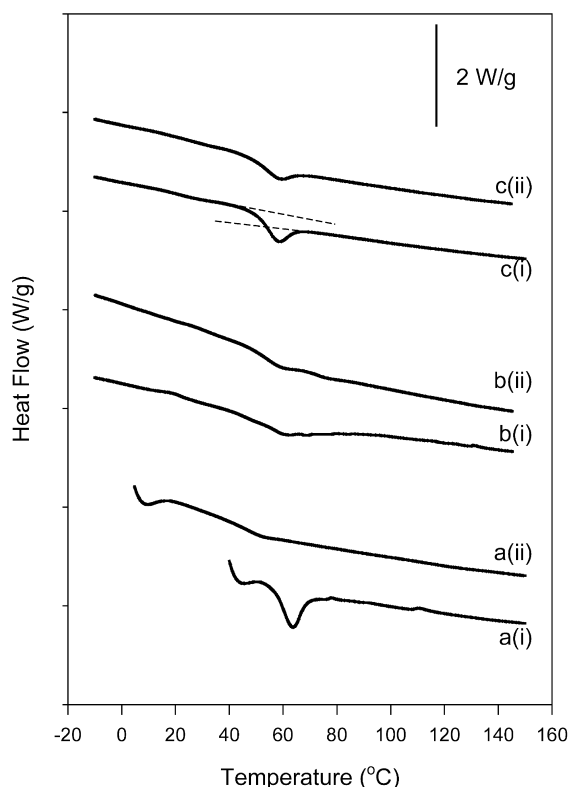


Fig. 6. Differential Scanning Calorimetry (DSC) characterization of POSS homopolymer, p(MA-POSS) using a heating rate of  $20^\circ\text{C}/\text{min}$  and with systematically varied thermal histories: a(i) the first scan, followed by a(ii), a second scan after directly cooling to  $0^\circ\text{C}$ ; b(i) a heating scan following a(ii) and subsequent annealing at  $T = 45^\circ\text{C}$  for 4 days, followed by b(ii), a heating scan after directly cooling to  $T = -10^\circ\text{C}$ ; c(i) a heating scan following b(ii) and subsequent annealing at  $T = 55^\circ\text{C}$  for seven days, followed by c(ii), a heating scan after directly heating to  $T = -10^\circ\text{C}$ . Traces are vertically displaced for clarity, but preserving the inset scale bar of  $2\text{ W/g}$ .

behavior. Annealing at a temperature closer to  $T_g$ , however, does result in the appearance of a slight endotherm at  $T_g$ , as shown in trace c (i) of Fig. 6. Here, annealing was conducted at  $T = 55^\circ\text{C}$  for seven days, resulting in a peak after  $T_g$  (onset  $T_g = 46.5^\circ\text{C}$ ) at  $T = 58^\circ\text{C}$ . This feature is largely erased on cooling and reheating without annealing (trace c (ii)), but not entirely.

By comparison of Figs. 5 and 6, we make the following salient observations: (i) the  $T_g$  for p(MA-POSS) homopolymer is 20–25  $^\circ\text{C}$  lower than that observed in a triblock copolymer bearing the same MA-POSS repeating unit (isobutyl corner groups), (ii) in both cases, enthalpy relaxation is indicated for thermal annealing at  $T < T_g$ , and (iii) enthalpy relaxation for p(MA-POSS) homopolymer is rapid only quite close to  $T_g$  in contrast to the triblock copolymer, where relaxation was indicated for annealing 40  $^\circ\text{C}$  below  $T_g$ . While we do not have a definitive explanation for this large  $T_g$  difference in aging behavior, recent studies by Zhu et al. [32] revealed an analogous sensitivity of PEO crystal stability on the matrix  $T_g$  of PEO/PS cylindrical diblocks. Specifically, it was observed on the

basis of DSC, WAXS, and SAXS analyses that PEO crystallization was enhanced for ‘soft confinement’; i.e. when the PS matrix was plasticized to a  $T_g < T_{\text{cryst.}}$  relative to crystallization within glassy PS confinement. It was argued that the enhanced stability for soft confinement is related to increased dimensionality (in the Avrami sense) of the crystals perhaps afforded by a mechanically compliant environment. We suggest an analogous explanation for the contrasting physical aging behavior between the p(MA-POSS) homopolymer (slow aging) and p(MA-POSS)<sub>10</sub>-*b*-pBA<sub>201</sub>-*b*-p(MA-POSS)<sub>10</sub> triblock (faster aging). While aging in the p(MA-POSS) homopolymer sample transpires in a rigid environment relatively devoid of surface or interface, the triblock copolymer ages with proximity to an interface with compliant pBA ( $T_g \sim -55^\circ\text{C}$ ). Recall from Fig. 4 that we observe a cylindrical morphology of continuous p(MA-POSS) and pBA cylinders; apparently, such a ‘soft confinement’ enhances the physical aging process while raising  $T_g$  significantly.

### 3.5. WAXS studies of triblock copolymers

To further elucidate the aging of the POSS containing homopolymer samples, we have examined the local structure of our polymers using WAXS and compare the results with scattering patterns of the POSS monomer and a triblock copolymer (p(MA-POSS)<sub>6</sub>-*b*-pBA<sub>481</sub>-*b*-p(MA-POSS)<sub>6</sub>) sample. The results are shown in Fig. 7. For reference, we show in trace (iv) the WAXS pattern for a representative MA-

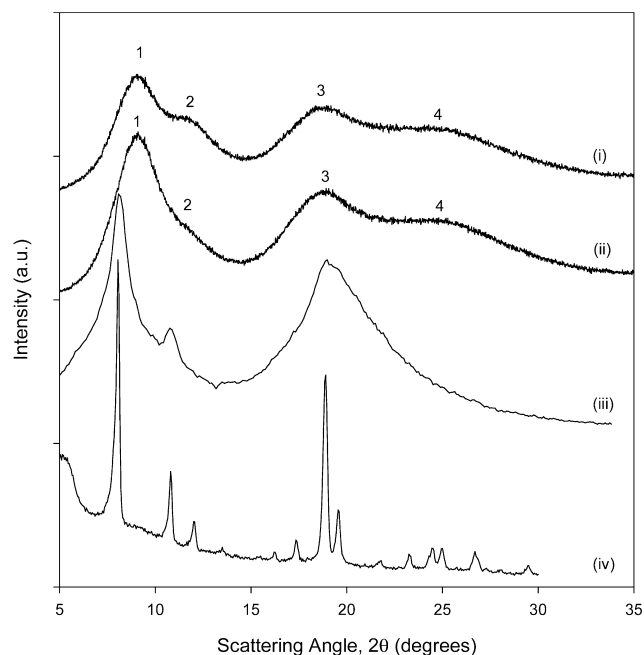


Fig. 7. Powder patterns of wide-angle X-ray scattering (WAXS) using Cu K $\alpha$  radiation ( $\lambda = 1.5418 \text{ \AA}$ ) for (i) p(MA-POSS) homopolymer following annealing at  $T = 55^\circ\text{C}$  for seven days (same as DSC trace c (i) for Fig. 5); (ii) p(MA-POSS) homopolymer as isolated after fractionation; (iii) POSS triblock copolymer, p(MA-POSS)<sub>6</sub>-*b*-pBA<sub>481</sub>-*b*-p(MA-POSS)<sub>6</sub>; and (iv) MA-POSS (cyclopentyl) monomer.

POSS monomer (R = cyclopentyl, others are virtually identical) revealing a rhombohedral unit cell by comparison with a previous report [4]. Polymerization yielding the p(MA-POSS) homopolymer, destroys crystallinity to leave four broad scattering peaks in the WAXS patterns (trace (ii)), one of which is sensitive to aging. In particular, the unaged sample (ii) shows very strong scattering at angles,  $2\theta = 9.12, 18.76^\circ$ , weak scattering at  $2\theta = 23.22 \text{ deg}$ , and very weak scattering near  $2\theta = 12 \text{ deg}$ . These peaks correspond grossly to the 101, 030, 312, and 110 *hkl* reflections of the rhombohedral unit cell of the POSS monomer [4], but with significant shift in the 101 and 110 reflections. We note that such comparison is not meant to suggest that this polymer is crystalline, nor that it would have the same unit cell as the monomer. Upon aging at  $T = 55^\circ\text{C}$  for seven days, as for the case of trace c (i) in Fig. 6, we observe near-doubling of the peak at  $11.27 \text{ deg}$  ( $110, 7.85 \text{ \AA}$ ) from 6.2% of the total wide-angle scattering to 12.4% (trace (i)), indicating some enhanced alignment of POSS ‘faces’ with respect to each other. Meanwhile, peaks 1 and 4 are observed to reduce in size while peak 4 also shifts to smaller *d*-spacing. Table 1 summarizes the WAXS data for the p(MA-POSS) homopolymer sample, with area-% being calculated using deconvolution with Peakfit™ software and assuming a Lorentzian form for each peak.

While beyond the scope of the present study, preliminary investigation of triblock microstructure by WAXS of both triblock copolymers has shown behavior intermediate between the high level of ordering in POSS monomer and low ordering of POSS homopolymer, but very similar to previously reported observations on POSS-based multi-block polyurethanes (Fig. 6) [4]. Trace (iii) of Fig. 7 shows a WAXS pattern typical of the triblocks, but in this case for p(MA-POSS)<sub>6</sub>-*b*-pBA<sub>481</sub>-*b*-p(MA-POSS)<sub>6</sub>.

### 3.6. Rheological behavior of triblock copolymers

Finally, we have characterized the rheological behavior of the microphase separated p(MA-POSS)<sub>10</sub>-*b*-pBA<sub>201</sub>-*b*-p(MA-POSS)<sub>10</sub> triblock copolymer using dynamic oscillatory shear for temperatures spanning  $80^\circ\text{C} < T < 170^\circ\text{C}$ ; i.e. above the softening points of both phases:  $T > T_g^{\text{p(MA-POSS)}} \gg T_g^{\text{pBA}}$ . Thus, Fig. 8 shows a

Table 1  
Analysis of WAXS patterns from Fig. 7

Peak	Original Sample		Annealing at $55^\circ\text{C}$ for one week	
	$2\theta$ (deg), <i>d</i> spacing ( $\text{\AA}$ )	Area (%) <sup>a</sup>	$2\theta$ (deg), <i>d</i> spacing ( $\text{\AA}$ )	Area (%) <sup>a</sup>
1	9.12 (9.71)	32.4	9.10 (9.72)	27.9
2	11.27 (7.85)	6.2	11.93 (7.42)	12.4
3	18.76 (4.73)	15.3	18.52 (4.79)	17.9
4	23.22 (3.83)	46.1	23.60 (3.77)	41.8

<sup>a</sup> Obtained by Lorentzian deconvolution.

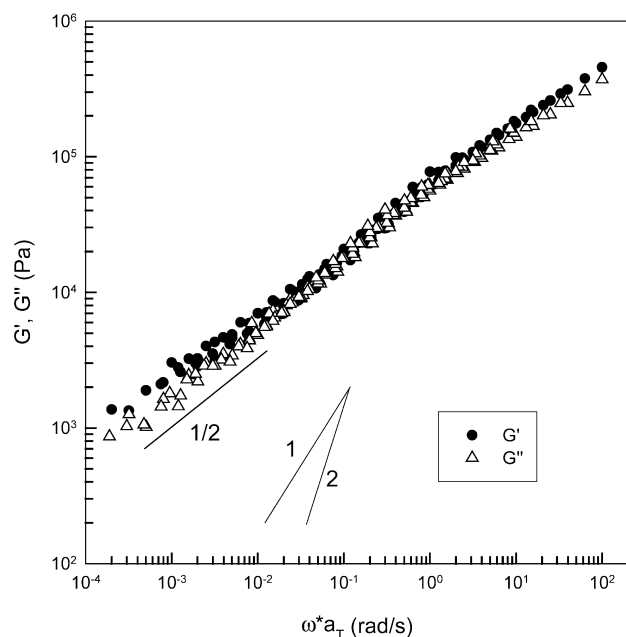


Fig. 8. Dynamic oscillatory shear data in the form of  $G'$  and  $G''$  master curves for tri-block copolymer  $p(\text{MA-POSS})_{10}\text{-}b\text{-}p(\text{BA})_{201}\text{-}b\text{-}p(\text{MA-POSS})_{10}$ ; The reference temperature for time-temperature superposition shifting was  $T = 80^\circ\text{C}$ .

master curve for shear storage and loss moduli where a reference temperature of  $T = 80^\circ\text{C}$  was used and frequency sweeps spanning  $0.1 < \omega < 100$  rad/s were collected over the stated temperature range. With reference to Fig. 3, the viscoelastic properties of the material beyond the sensitive range of DMA (i.e. at higher temperature) were examined by shear rather than tensile deformation, noting  $E' \sim 3G'$ . We observe modest applicability of TTS for our data, although this is not expected for microphase separated morphologies, with a lack of fluidity at even the highest temperatures and lowest frequencies probed. This can be seen clearly by comparison of the storage and loss modulus traces with the expected fluid scalings of  $G' \sim \omega^2$  and  $G'' \sim \omega$  shown as reference lines on the plot. Indeed, a slope near 1/2 is observed for the low frequency regions of both the storage and loss shear moduli. Such a response is consistent with other rheological observations for ordered block copolymers (Fig. 4) and implicates elasticity derived from the microphase separated morphology of a strongly segregated system [33]. We have observed no indication of an order-disorder transition in this system for  $T < 170^\circ\text{C}$ , the highest temperature probed in our experiments, but expect that  $T_{\text{ODT}}$  may be quite high due to the large incompatibility between the p(POSS-methacrylate) and p(butyl acrylate) phases.

#### 4. Conclusions

The synthesis and characterization of POSS containing homopolymers and ABA triblock copolymers was con-

ducted. ABA triblock copolymers possessing a soft middle pBA segment and outer p(MA-POSS) segments were prepared using ATRP. We demonstrate that optimization of composition and DP of each segment enabled the preparation of microphase separated structures, but with surprising morphologies. In particular, thin films of ABA triblock copolymers of  $p(\text{MA-POSS})_{10}\text{-}b\text{-}p(\text{BA})_{201}\text{-}b\text{-}p(\text{MA-POSS})_{10}$  were characterized using TEM to reveal the formation of a pBA cylinders in a p(MA-POSS) matrix. Thermal analysis indicated the presence of two clear glass transitions in the microphase-separated system with strong physical aging observed in samples annealed at temperatures near the  $T_g$  of the p(MA-POSS) phase. The occurrence of physical aging was further supported by wide-angle X-ray scattering indicating that rearrangement of POSS moieties was observed in glassy domains. It was found that the  $T_g$  of the p(MA-POSS) phase from triblock copolymers sequestered in microphase separated domains was nearly  $25^\circ\text{C}$  higher than a p(MA-POSS)-homopolymer of the comparable molar mass, suggesting a strong confinement-based enhancement of  $T_g$  in this system.

#### Acknowledgements

PTM acknowledges preliminary WAXS analysis performed by Dr Hong G. Jeon and financial support of AFOSR, Grant F49620-00-1-0100. The National Science Foundation under Grant No. PHY99-07949 (PTM), DMR 9871450 (KM) and Dr John Harrison, Legacy Fellowship at GMU, (JP) are gratefully acknowledged for funding of this research.

#### References

- [1] Pyun J, Matyjaszewski K. *Chem Mater* 2001;13:3436–48.
- [2] Phillips SH, Blanski RL, Svejda SA, Haddad TS, Lee A, Lichtenhan JD, Feher FJ, Mather PT, Hsiao BS. *Mater Res Soc Symp Proc* 2001; 628:CC461–CC4610.
- [3] Haddad TS, Lee A, Phillips SH. *Polym Prepr (Am Chem Soc, Div Polym Chem)* 2001;42:88–9.
- [4] Fu BX, Hsiao BS, Pagola S, Stephens P, White H, Rafailovich M, Sokolov J, Mather PT, Jeon HG, Phillips S, Lichtenhan J, Schwab J. *Polymer* 2000;42:599–611.
- [5] Fu BX, Zhang W, Hsiao BS, Johansson G, Sauer BB, Phillips S, Blanski R, Rafailovich M, Sokolov J. *Polym Prepr (Am Chem Soc, Div Polym Chem)* 2000;41:587–8.
- [6] Mather PT, Jeon HG, Romo-Uribe A, Haddad TS, Lichtenhan JD. *Macromolecules* 1999;32:1194–203.
- [7] Jeon HG, Mather PT, Haddad TS. *Polym Int* 2000;49:453–7.
- [8] Zheng L, Farris RJ, Coughlin EB. *J Polym Sci, Part A: Polym Chem* 2001;39:2920–8.
- [9] Zheng L, Farris RJ, Coughlin EB. *Macromolecules* 2001;34:8034–9.
- [10] Haddad TS, Choe E, Lichtenhan JD. *Mater Res Soc Symp Proc* 1996; 435:25–32.
- [11] Lichtenhan JD, Otonari YA, Carr MJ. *Macromolecules* 1995;28: 8435–7.
- [12] Matyjaszewski K, editor. *Controlled Radical Polymerization*.

- Proceedings of a Symposium at the 213th National Meeting of the American Chemical Society, held 13–17 April 1997; San Francisco, California. ACS Symp Ser, 1998; 685: 1998; p. 483.
- [13] Matyjaszewski K, editor. Controlled/Living Radical Polymerization. Progress in ATRP, NMP, and RAFT. Proceedings of a Symposium on Controlled Radical Polymerization held on 22–24 August 1999; New Orleans. ACS Symp Ser, 2000; 768: 2000; p. 484.
- [14] Matyjaszewski K. *Macromol Symp* 2001;174:51–67.
- [15] Wang J-S, Matyjaszewski K. *J Am Chem Soc* 1995;117:5614–5.
- [16] Pyun J, Matyjaszewski K. *Macromolecules* 2000;33:217–20.
- [17] Matyjaszewski K, Xia J. *Chem Rev (Washington, DC)* 2001;101:2921–90.
- [18] Patten TE, Matyjaszewski K. *Accounts Chem Res* 1999;32:895–903.
- [19] Romo-Uribe A, Mather PT, Haddad TS, Lichtenhan JD. *J Polym Sci, Part B: Polym Phys* 1998;36:1857–72.
- [20] Fu BX, Hsiao BS, White H, Rafailovich M, Mather PT, Jeon HG, Phillips S, Lichtenhan J, Schwab J. *Polym Int* 2000;49:437–40.
- [21] Fu BX, Yang L, Somani RH, Zong SX, Hsiao BS, Phillips S, Blanski R, Ruth P. *J Polym Sci, Part B: Polym Phys* 2001;39:2727–39.
- [22] Haddad TS, Mather PT, Jeon HG, Chun SB, Phillips SH. *Mater Res Soc Symp Proc* 2001;628:CC2.6.1–CC2.6.7.
- [23] Tant MR, Wilkes GL. *Polym Engng Sci* 1981;21:325–30.
- [24] Matyjaszewski K, Patten TE, Xia J. *J Am Chem Soc* 1997;119:674–80.
- [25] Buchowicz W, Holerca MN, Percec V. *Macromolecules* 2001;34:3842–8.
- [26] Bharadwaj RK, Berry RJ, Farmer BL. *Polymer* 2000;41:7209–21.
- [27] Tong J-D, Jerome R. *Macromolecules* 2000;33:1479–81.
- [28] Fujino K, Senshu K, Kawai H. *J Colloid Sci* 1961;16:262.
- [29] Wu S. *J Polym Sci Polym Phys Ed* 1989;27:723.
- [30] Kim GM, Sun F, Fang X, Qin H, Mather PT, In preparation. 2002.
- [31] Brandrup J, Immergut EH, Grulke EA. *Polymer Handbook*, 4. New York: Wiley Interscience; 1999.
- [32] Zhu L, Mimnaugh BR, Ge Q, Quirk RP, Cheng SZD, Thomas EL, Lotz B, Hsiao BS, Yeh F, Liu L. *Polymer* 2001;42:9121–31.
- [33] Larson RG. *The Structure and Rheology of Complex Fluids*. New York: Oxford University Press; 1999. Chapter 13.